Battery charging system for PHEV and EV using single phase AC/DC PWM buck converter

Keun-Young Kim
University of Sungkyunkwan
300 Cheoncheon-dong, Jangan-gu, Suwon, Gyeonggi-do, Korea
Kimky.jh@gmail.com

Sang-Hoon Park
University of Sungkyunkwan
300 Cheoncheon-dong, Jangan-gu, Suwon, Gyeonggi-do, Korea
marohachi@skku.edu

Seung-Kyung Lee
University of Sungkyunkwan
300 Cheoncheon-dong, Jangan-gu, Suwon, Gyeonggi-do, Korea
Lsk731@skku.edu

Taeck-Kie Lee
National University of HanKyong
167 Chungang-ro Anseong-si Gyeonggi-do, Korea
tklee@hknu.edu

Chung-Yuen Won
Senior member, IEEE
Univ. of Sungkyunkwan
300 Cheoncheon-dong, Jangan-gu, Suwon, Gyeonggi-do, Korea
won@yurim.skku.ac.kr

***Abstract*- In this paper, a battery charging system for Plug-in Hybrid Electric Vehicle (PHEV) and Electric Vehicle (EV), and operation algorithm of charging system is introduced. Also, the proposed charging system uses commercial electricity in order to charge the battery of parked PHEV, and 48*V* battery charging system with power factor controllable single phase converter for PHEV is investigated in this paper. This research verifies the power factor control of input and the converter output controlled by the charge control algorithm through simulation and experiment.**

***Keywords:* Plug-in Hybrid Electric Vehicle, Electric Vehicle, Battery charge, AC-DC PWM buck converter, CC-CV.**

I. INTRODUCTION

Recently, as regulation of the environment being strengthened, developed countries have started reducing pollutants. So, most countries restrict to spend products consuming fossil fuel and research into alternative energy sources. Therefore, Japan, U.S. and many European countries stand at the head for developing environmental friendly vehicle. Globally advanced nation vehicle companies continuously invest to develop Hybrid Electric Vehicle using a battery and electric motor as an auxiliary power system. Since fuel cell and Electric Vehicle technology face technical difficulty, the investigation of Plug-in Hybrid Electric Vehicle is in spotlight recently.

Comparing to conventional Hybrid Electric Vehicle, the battery attached in Electric Vehicle and Plug-in Hybrid Electric Vehicle is charged through using the plug linked to grid and a external charger [9], [10]. Moreover, Plug-in Hybrid Electric Vehicle is not only having low ratio of fuel consumption but also environmental friendly characteristics because electric power operates the vehicle. Especially, battery charger using conventional power source and inverter for controlling the electric motor of Plug-in Hybrid Electric Vehicle would be developed necessarily

Plug-in Hybrid Electric Vehicle has same structure as Hybrid Electric Vehicle. Plug-in Hybrid Electric Vehicle, however, operates with the battery which is charged through commercial electricity 220*V*. Especially, Plug-in Hybrid Electric Vehicle reduces the use of fossil fuel engine and increases the driving force from electrical motor [9], [10].

The battery charging system proposed in this research consists of power conversion system based on single phase buck converter [1]-[5]. The controller is able to control power factor [6], [7] and has a battery charging system algorithm [8]. The performance of the control is verified through simulation and experiment.

II. SINGLE PHASE AC/DC PWM BUCK CONVERTER

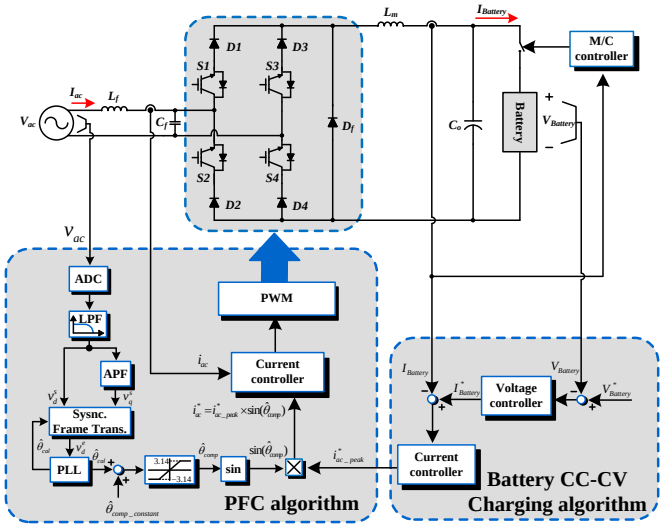

Fig. 1. Topology and control block diagram of single phase AC/DC PWM buck converter.

Fig. 1 is the topology of single phase AC/DC PWM buck converter and the block diagram of control in this paper [1]-[3]. The composition of semiconductor switch is bridge type. Compared to a conventional single phase converter, the converter in this research has different switch and diode composition. Although the composition of each switch and diode is different, the operation of the circuit is similar to buck converter [1]-[3].

Fig. 2 represents the equivalent circuit block diagram of the operation modes in single phase AC/DC PWM buck converter [4], [5].

978-1-4244-8218-4/10/$26.00 ©2010 IEEE

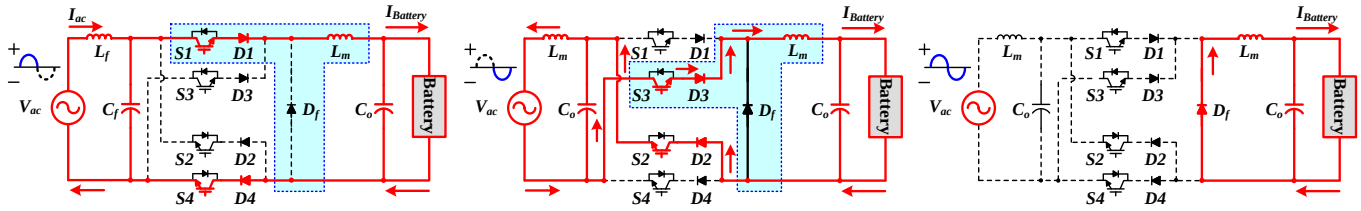

(a) Mode 1 (b) Mode 2 (c) Mode 3

Fig. 2. Equivalent circuit block diagram of the operation modes in single phase AC/DC PWM buck converter.

Mode 1 (Fig. 2–(a)) – For half a cycle of positive of input voltage, Mode 1 is operated through commercial electricity 220*V* of input terminal. When switches *S1* and *S4* are turn on, mode 1 begins. The energy of input voltage is transferred to load through switches (*S1*, *S4*) and diodes (*D1*, *D4*).

Mode 2 (Fig. 2-(b)) – For half a cycle of negative of input voltage, mode 2 is operated through commercial electricity 220*V* of input terminal. When switches *S2* and *S3* are turn on, mode 2 begins. The energy of input voltage is transferred to load through switches (*S2*, *S3*) and diodes (*D2*, *D3*).

Mode 3 (Fig. 2-(c)) – When all of switches are turned off, mode 3 is operated in freewheeling. The stored energy of main inductor (L_m) is transferred to load through diode (D_f), or capacitor (C_o).

III. DESIGN PROCEDURE

Fig. 3 shows the block diagram of input L-C filter which is attached to input terminal for power factor correction (PFC) [11].

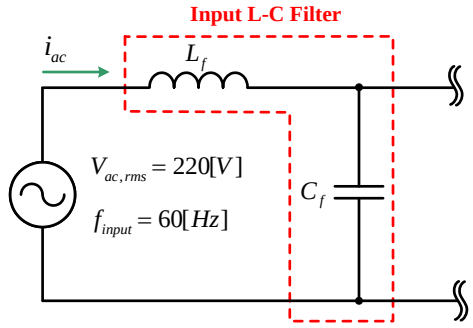

Fig. 3. Equivalent circuit block diagram of the input L-C filter.

In this case the maximum resonant frequency ($f_{r,max}$) is equal to half a switching frequency by (1). The resonant frequency (f_r) is given by (2).

$$f_{r,\max} = 0.5\times f_{sw} \tag{1}$$

$$f_r = 0.8\times f_{r,\max} = 0.8\times 0.5\times 10000 = 4[kHz] \tag{2}$$

A. *Inductor (L_f) of input L-C filter*

Input impedance is selected to consider the rms of input voltage ($V_{ac,rms}$) and battery charging system rating. The impedance is given by (3).

$$Z = \frac{(V_{ac,rms})^2}{P} = \frac{220^2}{1200} = 40.33[\Omega] \tag{3}$$

Designed impedance of filter inductor is smaller than whole impedance. In this research, the impedance of inductor (Z_{Lf}) is designed to 5% of whole impedance by (4). Therefore, inductance of filter inductor is given by (5) and (6).

$$Z_{L_f} = 40.33\times 0.05 = 2.0166[\Omega] \tag{4}$$

$$Z_{L_f} = 2\pi f_{input}\times L_f \tag{5}$$

$$L_f = \frac{2.01666}{2\times 3.14\times 60} \approx 5.35[mH] \tag{6}$$

B. *Capacitor(C_f) of input L-C filter*

The inductor (L_f) and capacitor (C_f) of input L-C filter is expressed by (2) and (6). Therefore, (7) must be satisfied. The capacitor (C_f) of input L-C filter is given by (8).

$$2\pi f_r = 2\times 3.14\times 4000 = \frac{1}{\sqrt{L_f C_f}} \tag{7}$$

$$C_f = \frac{1}{(2\pi f_r)^2\times L_f} = \frac{1}{(2\times 3.14\times 4000)^2\times 0.005} \approx 0.32[\mu F] \tag{8}$$

C. *Inductors (L_m) of output filter*

Inductor (L_m) of output filter is expressed by (9). Therefore, (10) must be satisfied. Inductor (L_m) in output filter is given by (10).

$$L_m = \frac{t_{on}}{\Delta I_L}(V_{ac,avg} - V_{Battery}) \ , (t_{on}: \text{switch on time}) \tag{9}$$

$$L_m = \frac{40\times 10^{-6}[\text{sec}]}{1[A]}\times(209[V]-51[V]) \approx 6.5[mH] \tag{10}$$

D. Devices of Switch (S1~S4) and diode (D1~D4 and D_f)

Switches (*S1~S4*) and diodes (*D1~D4* and D_f) are selected higher than rating in order to allow for surge voltage and current. In addition, diodes (*D1~D4* and D_f) are selected to consider reverse recovery time of the switch, also reverse recovery time of the diodes (*D1~D4* and D_f) are faster than reverse recovery time of the switches (*S1~S4*).

IV. SYSTEM CONTROL ALGORITHM

A. PLL algorithm

Fig. 4 shows a general structure of single-phase PLL (Phase-Looked Loop) with All-Pass Filter and synchronous frame transformation.

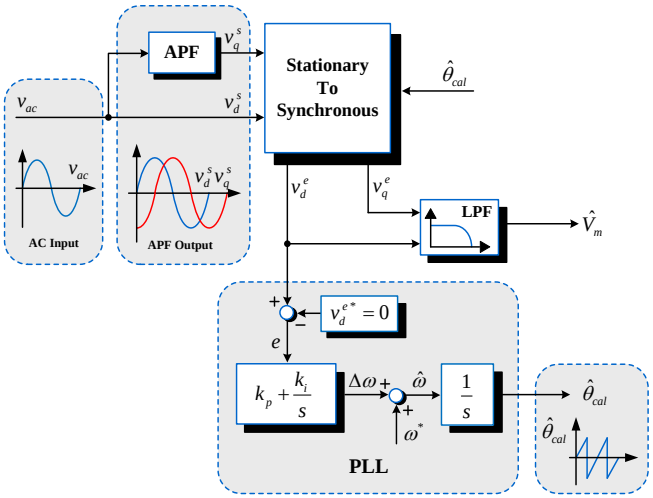

Fig. 4. A general structure of single-phase PLL with All-Pass Filter and synchronous frame transformation.

v_q^s is obtained through APF with input voltage v_{ac} and it is delayed PI/2 phase than input voltage. v_d^s and v_q^s are changed to the direct values v_d^e and v_q^e by synchronous frame transformation. The following (11~12) are the stationary to synchronous frame transformations.

$$v_d^e = v_d^s \cos\hat{\theta} + v_q^s \sin\hat{\theta} \tag{11}$$

$$v_q^e = -v_d^s \sin\hat{\theta} + v_q^s \cos\hat{\theta} \tag{12}$$

v_d^e and v_d^{e*} are the input of single-phase PLL controller and then PI-compensator generates $\Delta\omega$. $\Delta\omega$ is the estimation phase error of input voltage. $\hat{\omega}$ is sum of $\Delta\omega$ and ω^*. $\hat{\theta}_{cal}$ is calculated by the integration of $\hat{\omega}$.

B. Theta ($\hat{\theta}$) compensator

When, data transferred from sensor to controller through ADC (Analog to Digital Conversion), the problem can occurs as error by noise characteristics.

In this research, digital LPF (Low-Pass Filter) is used in order to reduce noise characteristics at AD conversion of input v_{ac}. Although it enables to diminish noise characteristics, unfortunately phase delay is unavoidable. So it is necessary to need theta compensator.

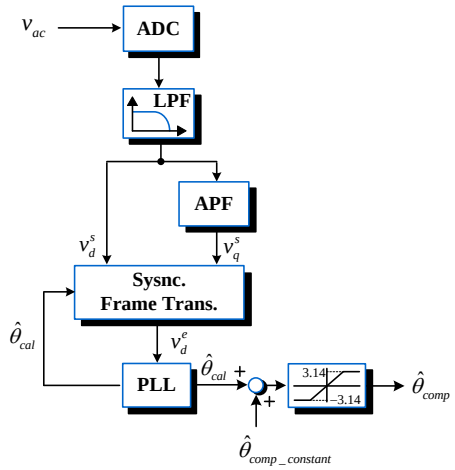

Fig. 5. Control block diagram of theta compensator in PLL.

Fig. 5 shows the control block diagram of theta $\hat{\theta}$ compensator in PLL algorithm. $\hat{\theta}$ is obtained through LPF and is used synchronous frame transformations and PLL control block. The error value of $\hat{\theta}$ is compensated because $\hat{\theta}_{\text{comp-constant}}$ is add to $\hat{\theta}$. Finally, $\hat{\theta}_{\text{comp}}$ is limited to that both 3.14 and -3.14 by limiter.

B. Battery CC-CV charging control algorithm

The control algorithm for constant current and constant voltage is shown in Fig. 6. In constant current control, when battery voltage is reached to design charging voltage, the control method changed to constant voltage control method to make the charging voltage stable, and the charging current amount of flowing current is getting decreased simultaneously.

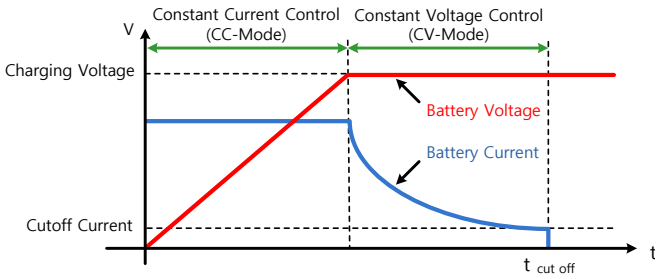

Fig. 6. The general method has constant current control and constant voltage control of the battery charging control algorithm.

Moreover, when the current is equal to that of cut-off current, whole charging of control system operation is ended, and the energy is transferred from input to battery should be shut down.

If the control is running when the current has same value as that of cut-off, the voltage of the battery of increasing, and the voltage are over the maximum voltage limit.

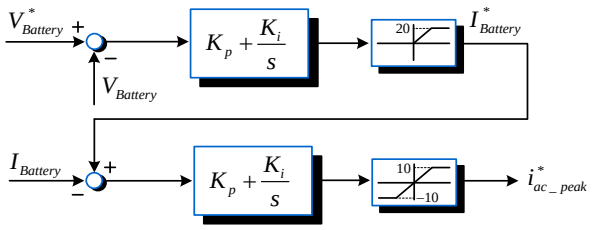

Fig. 7. Control block diagram of battery CC-CV charging algorithm.

Fig. 7 is control block diagram of battery CC-CV charging algorithm [6]. Two PI-controller (K_p+K_i/s) are used for to CC control and CV control.

CV control is composed of battery voltage $V_{Battery}$, battery voltage reference $V^*_{Battery}$, two PI-controller and limiter. A difference in values between battery voltage and battery voltage reference is through PI-controller. Battery current reference $I^*_{Battery}$ is generated by CV controller and is limited to 20[A]

CC control consists of battery current, battery current reference, PI-compensator and limiter. A difference in values between battery current and battery current reference is through PI-compensator. Peak reference value of input current $i^*_{ac\text{-}peak}$ is generated by CC control. Maximum peak reference value of input current is limited 10A as well as minimum peak reference value of current is limited -10A at input terminal.

C. *PFC algorithm*

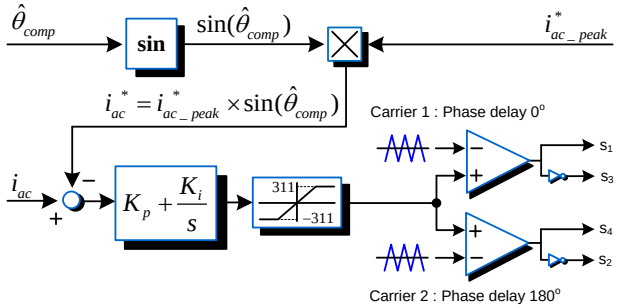

Fig. 8. Control block diagram of PFC algorithm.

Fig. 8 shows control block diagram of PFC algorithm in input terminal. Unit sine wave is obtained by compensated theta $\hat{\theta}_{comp}$ and sine function. Input current reference i^*_{ac} is generated by multiplying peak reference value of input current and unit sine wave.

A difference in values between input real current i_{ac} and input current reference is through PI-controller. Maximum reference value of voltage is limited 311V as well as minimum reference value of voltage is limited -311V at input terminal. Finally, 4 PWM signals (S_1~S_4) are generated through two comparators [6], [7].

V. SIMULATION

The performance of a 1.2kW, single phase shift AC/DC PWM buck converter was designed to the following specifications in Table I. This paper was simulated the battery charging system by POWERSIM Inc. PSIM software.

Table I
Parameter values of The Battery Charging System.

Input Voltage.	V_{ac}	$220V_{rms}$
Output Voltage.	$V_{Battery}$	50.7V
Output Current.	$I_{Battery}$	20A
Switching Freq.	f_s	10kHz
Input Filter Inductor.	L_f	5.5mH
Input Filter Capacitor.	C_f	0.32μF
Output Filter Inductor.	L_m	6.5mH
Output Capacitor.	C_o	7100μF

And System is used the battery and the battery bank to simulation and experiment with following specifications in Table II.

Table II
Parameter values of battery bank.

Battery Model.	DELKOR Hi-Ca 100 (Lead-Acid)	
Nominal Voltage.	12V	
Typical Capacity.	100Ah	
Charge Condition.	Max. Current.	20A
	Max. Voltage.	14.5 ~ 14.8V
Discharge Condition.	Continuous Current.	80A
	Max. Current.	200A
	Cut-Off Voltage.	11.4V
Life Cycle.	> 2500 Cycle @ 80% DoD	
Battery Bank Construction (12[V]×4EA=48[V]).	Charging Voltage.	50.7V
	Charging Current.	20A
	Cut-Off Current.	2A
	Max. Allowable Voltage.	53.3V

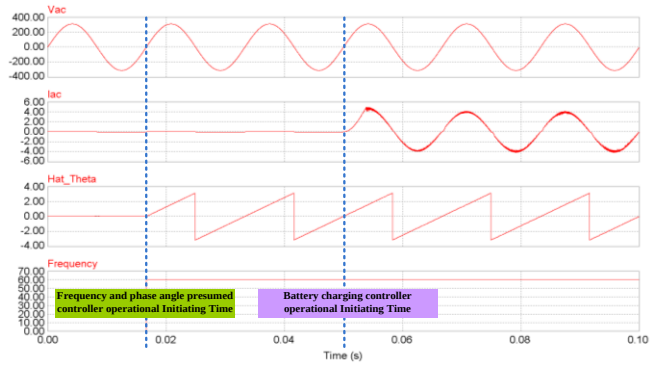

Fig. 9. Simulation results of the input voltage, input current, frequency and phase angle of input voltage.

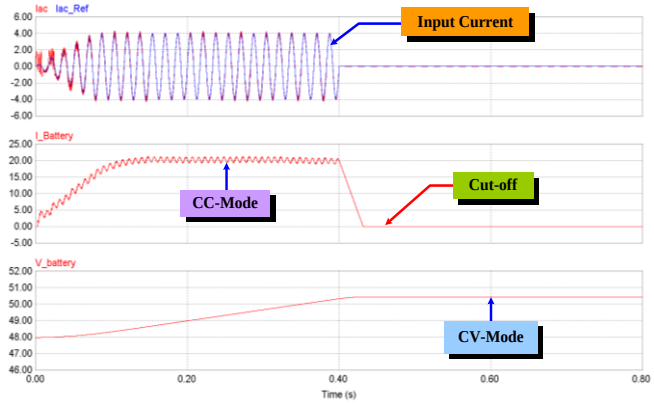

Fig. 10. Simulation results of the input current, battery current and battery voltage.

In Fig. 9, starting point of PLL control is one period delayed point after input voltage sensing. After that time, the operating time for battery charging control can be arbitrary determined.

Fig.10 shows the constant current control and the constant voltage control. During the constant current control period, the battery voltage is gradually increasing. When the battery voltage is equal to 48*V*, the constant voltage control begins, but the battery voltage is controlled to reach 50.7*V*. At this point, the charging current decreases rapidly to cut-off current (commonly 2*A*, in lead battery).

After the some amount of time, the charging control operation is ended to prevent the battery voltage from being overcharged that is a maximum voltage limit, in case of long-term negligence.

VI. EXPERIMENTAL RESULT

Fig.11 is the whole composition of battery charging system for 1.2*kW* experiment in this paper. It is composed of converter, sensors, input/output filter, gate driver & SMPS, heat sink. The controller of battery charging system is based on DSP *TMS320F28335*. Commercial electricity 220*V* is connected to the input terminal of the power conversion system through the input LC filter. The converted energy is injected to the battery through the output filter inductor, the output capacitor and M.C (MC state of turn-on)

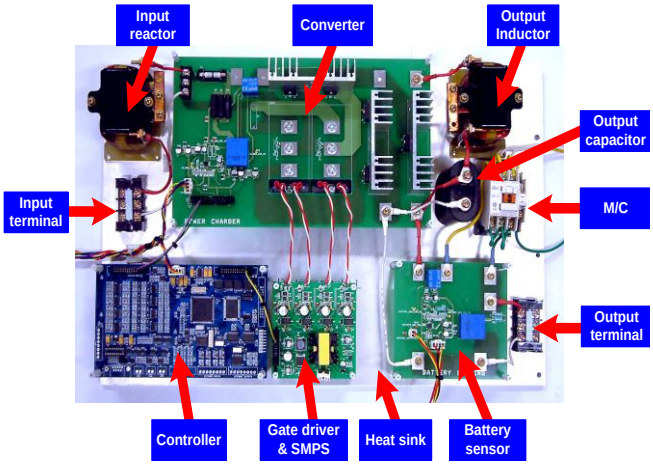

Fig. 11. Battery charging system.

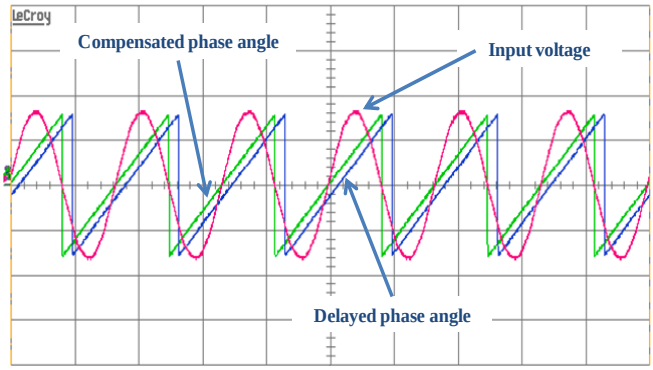

Fig. 12. Experimental results of input voltage and delayed and compensated phase angle.
(Input voltage; Y-axis = 200[V/div.], Delayed and compensated phase angle; Y-axis = 2[V/div], X-axis = 10[ms/div.])

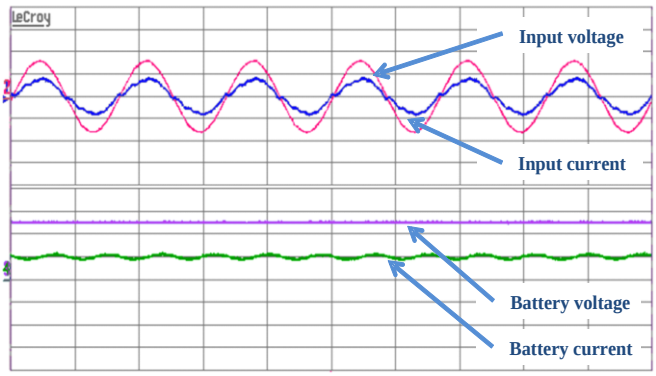

Fig. 13. Experimental results of input voltage, input current and battery voltage.
(Input voltage; Y-axis = 200[V/div.], Input current; Y-axis = 4[A/div], Battery voltage; Y-axis = 20V/div.], Battery current; Y-axis = 20[A/div.], X-axis = 10[ms/div.])

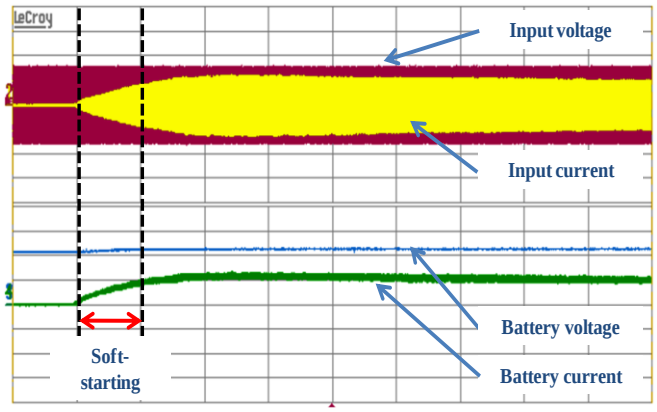

Fig. 14. Experimental results of input voltage, Input current, battery voltage and current in initial constant current mode.
(Input voltage; Y-axis = 200[V/div.], Input current; Y-axis = 4[A/div], Battery voltage; Y-axis = 20[V/div.], Battery current; Y-axis = 20[A/div.], X-axis = 2[s/div.], Battery initial voltage = 44[V])

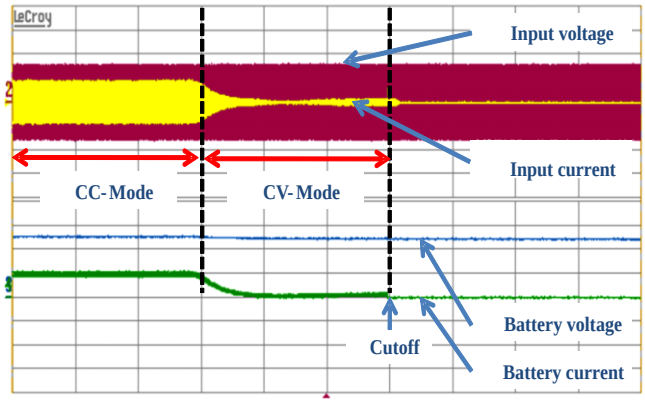

Fig. 15. Experimental results of input voltage, input current, battery voltage and current in constant voltage mode.
(Input voltage; Y-axis = 200[V/div.], Input current; Y-axis = 4[A/div], Battery voltage; Y-axis = 20[V/div.], Battery current; Y-axis = 10[A/div.], X-axis = 2[s/div.], Battery charging voltage = 50.7[V])

Fig.12 shows the experimental results of the input voltage, and compensated phase angle, delayed phase angle. The phase angle is compensated to input phase angle.

Fig.13 shows the experimental results of the input voltage, current and the battery voltage. It shows that the input voltage and current are in phase and also that the power factor control is well performed.

Fig.14 shows the experimental results of the input voltage, input current. In experiment, the battery charging voltage is controlled by soft starting to prevent the overshoot at the initial of steady state

Fig.15 shows the experimental results of the input voltage, input current, battery voltage and current in CC-Mode and CV-Mode. In experiment, the battery charging is controlled by CC-Mode to CV-Mode. When battery voltage is reached to design charging voltage, the CC-Mode operation is ended to prevent the battery voltage from being overcharged at Cutoff time.

VII. CONCLUSION

The proposed battery charging system in this research consists of power conversion system based on single phase buck converter. It is non-isolation type converter and has one stage composition. The prototype battery charging system is designed for 48*V* battery of 1.2*kW* system of Plug-in Hybrid Electric Vehicle. Because of one stage structure, it has characteristic of miniaturization and light-weight. It is suitable as the household system. The performance of PFC algorithm in input terminal verifies through simulation and experiment. And battery charging algorithm is verified that the constant current control and constant voltage control are well performed.

In future, for optimized value for design, battery charging system will be added researches about characteristic analysis of the L-C filter and reactor.

ACKNOWLEDGMENT

This work is the outcome of a Manpower Development Program for Energy & Resources supported by the Ministry of Knowledge and Economy (MKE).

REFERENCES

[1] Ramesh Oruganti, Moorthi Palaniapan, “Inductor voltage controlled variable power factor buck-type AC-DC converter,” 27th Annual IEEE Power Electronics Specialists Conference, Vol. 1, pp.230-237, Jun 1996.

[2] Ramesh Oruganti, Moorthi Palaniapan, “Enhanced control design of single phase AC-DC converter using power balance calculator,” 4th International Power Electronics and Motion Control Conference, Vol. 3, pp. 1101-1104, Aug 2004.

[3] Ramesh Srinivasan, Moorthi Palaniapan, Ramesh Oruganti, “A Single Phase Two-Switch Buck Type AC-DC Converter Topology with Inductor Voltage Control,” 28th Annual IEEE Power Electronics Specialists Conference, Vol. 1, pp. 556-563, Jun 1997.

[4] Ramesh Oruganti, Moorthi Palaniapan, “Inductor Voltage Control of Buck-Type Single-Phase AC–DC Converter,” *IEEE Transactions on power electronics*, Vol. 15, No. 2, pp.411-416, May 2000.

[5] Bhim Singh, Brij N. Singh, Ambrish Chandra, Kamal Al-Haddad, Ashish Pandey, and Dwarka P. Kothari, “A Review of Single-Phase Improved Power Quality AC-DC Converters,” *IEEE Transactions on Industrial Electronics*, Vol. 50, No.8, pp.962-981, Oct 2003.

[6] Michael G. Egan, Dara L. O’Sullivan, John G. Hayes, Michael J. Willers,Christopher P. Henze, “Power-Factor-Corrected Single-Stage Inductive Charger for Electric Vehicle Batteries,” *IEEE Transactions on Industrial Electronics*, Vol. 54, No. 2, pp.1217-1226, Apr 2007.

[7] Ramesh Oruganti, Ramesh Srinivasan, “Single phase power factor correction - A review,” *Sadhana*, Vol. 22, Part 6, , pp. 753-780, Dec 1997.

[8] Chanakya B. Bhatt, Vinod P. Patel and Nimit K. Sheth, “High Voltage Battery Charger,” International Conference on Electrical Machines and Systems 2007, pp.1772-1777, Oct 2007.

[9] Young-Joo Lee, Alireza Khaligh, Ali Emadi, “Advanced Integrated Bidirectional AC/DC and DC/DC Converter for Plug-In Hybrid Electric Vehicles,” *IEEE Transactions on vehicular technology*, Vol. 58, No. 8, pp.3970-3980, Oct 2009.

[10] Ali Emadi, Young Joo Lee,Kaushik Rajashekara, “Power electronics and motor drives in electric, hybrid electric, and plug-in hybrid electric vehicles,” *IEEE Transactions on Industrial Electronics*, Vol. 55 , No.6, pp.2237-2245, Jun 2008.

[11] Chen Xiyon Yan Bin,Gao Yu, “The Engineering design and optimization of inverter output RLC filter in AC motor drive system,” IECON02, Vol.1, pp.175-180, 2002.